MOLECULAR AND CELLULAR BIOLOGY, Aug. 2001, p. 5624–5630 Vol. 21, No. 16
0270-7306/01/$04.00+0 DOI: 10.1128/MCB.21.16.5624–5630.2001

Preserved Pancreatic β-Cell Development and Function in Mice Lacking the Insulin Receptor-Related Receptor

TADAHIRO KITAMURA,[1] YOSHIAKI KIDO,[1] SERGE NEF,[2] JUSSI MERENMIES,[2] LUIS F. PARADA,[2] AND DOMENICO ACCILI[1]*

Naomi Berrie Diabetes Center and Department of Medicine, College of Physicians & Surgeons of Columbia University, New York, New York 10032,[1] and Center for Developmental Biology, University of Texas Southwestern Medical Center, Dallas, Texas 75390-9133[2]

Received 10 January 2001/Returned for modification 5 March 2001/Accepted 15 May 2001

Receptors of the insulin/insulinlike growth factor (IGF) family have been implicated in the regulation of pancreatic β-cell growth and insulin secretion. The insulin receptor-related receptor (IRR) is an orphan receptor of the insulin receptor gene (*Ir*) subfamily. It is expressed at considerably higher levels in β cells than either insulin or IGF-1 receptors, and it has been shown to engage in heterodimer formation with insulin or IGF-1 receptors. To address whether IRR plays a physiologic role in β-cell development and regulation of insulin secretion, we have characterized mice lacking IRR and generated a combined knockout of *Ir* and *Irr*. We report that islet morphology, β-cell mass, and secretory function are not affected in IRR-deficient mice. Moreover, lack of IRR does not impair compensatory β-cell hyperplasia in insulin-resistant $Ir^{+/-}$ mice, nor does it affect β-cell development and function in $Ir^{-/-}$ mice. We conclude that glucose-stimulated insulin secretion and embryonic β-cell development occur normally in mice lacking *Irr*.

In its simplest formulation, diabetes results from the inability of pancreatic β cells to maintain adequate insulin levels and prevent hyperglycemia. In type 1 diabetes, β-cell failure is caused by immune mechanisms, whereas in type 2 diabetes, it results from a combination of genetic and environmental causes (6, 33). It is generally agreed that insulin resistance is the main metabolic abnormality in type 2 diabetes and that it predisposes to β-cell failure (16, 41). The mechanism by which this occurs remains obscure. Based on observations in genetically engineered mice lacking various components of the insulin/insulinlike growth factor (IGF) signaling pathway, it has been proposed that insulin and IGF receptors regulate two key processes in the life of a β cell: proliferation and hormone secretion. Kulkarni et al. showed that ablation of *Ir* in β cells by site-specific recombination leads to altered glucose sensing and impairs glucose tolerance (22). A similar phenotype results from generalized ablation of *Irs*-1, a key molecule in insulin signaling (23). These data are consistent with the model proposed by Leibiger et al., in which insulin secretion provides a positive feedback regulation of insulin gene transcription (25). On the other hand, it has been shown that ablation of *Irs*-2 impairs β-cell growth in mice in a strain-dependent manner (21, 48) and that this phenotype is exacerbated by *Igf1r* haploinsufficiency, leading Withers and coworkers to propose that IGF-1R signaling through IRS-2 is required for β-cell growth (47).

IRR is an orphan receptor of the *Ir* family (39) which does not bind insulin or insulinlike peptides (14, 20, 49) and can be expressed as variably spliced isoforms (12). The tissue distribution of the *Irr* product is more restricted than that of either *Ir* or *Igf1r* (4, 24, 32, 34, 35, 40, 42–44, 46). In the kidney, the organ with the highest levels of *Irr* mRNA (24, 27, 34), IRR immunoreactivity has been detected in non-A intercalated cells (4, 32). In neural tissues, *Irr* expression is preferentially found in colinergic neurons of rat forebrain (42, 43) and in sympathetic and sensory neurons (34), where it appears to colocalize with TrkA receptors in nerve growth factor-positive neurons (35, 42). In the stomach, *Irr* mRNA is found in enterocromaffin cells (44).

Irr is also expressed in pancreatic islets, where it localizes to β cells (10, 31). Hirayama et al. reported that *Irr* mRNA is more abundant than either *Ir* or *Igf1r* mRNA in β cells and that its protein product is preferentially expressed as unprocessed precursor (10).

The function of IRR is unknown. Holodimeric IRR expressed in NIH 3T3 cells can be activated by vanadate (14), and heterodimeric IR/IRR receptors can be activated by insulin to phosphorylate IRS-1 and IRS-2, providing proof of principle of the signaling abilities of its kinase (10, 49). Similarly, a chimeric TrkB/IRR receptor can induce mitogen-activated protein (MAP) kinase activity in PC-12 cells and promote neurite outgrowth, in contrast to IR activation, which induces proliferation (17). Because IRR has been shown to engage in heterodimer formation with both IR and IGF-1R (13, 20), it is possible that it functions by modulating IR and/or IGF-1R signaling in either a positive or negative manner (37). The latter possibility is especially appealing to explain IRR function in β cells, where hybrid IR/IRR receptors may provide a mechanism to prevent a constitutive state of insulin-induced IR phosphorylation and downregulation. It is unclear, in fact, how IR and IGF-1R may be regulated in the β cell, in view of the fact that IR is presumably exposed to high insulin concentrations in the pancreatic portal circulation and that IGF-1 has been shown to inhibit insulin secretion (50).

To address these questions, we have studied the effects of nullizygous *Irr* mutations on β-cell development and secretory function and generated mice lacking both *Ir* and *Irr* to study the effect of the *Irr* mutation in a diabetes-predisposing background.

* Corresponding author. Mailing address: Russ Berrie Science Pavilion, 1150 St. Nicholas Ave., New York, NY 10032. Phone: (212) 304-7393. Fax: (212) 304-7390. E-mail: da230@columbia.edu.

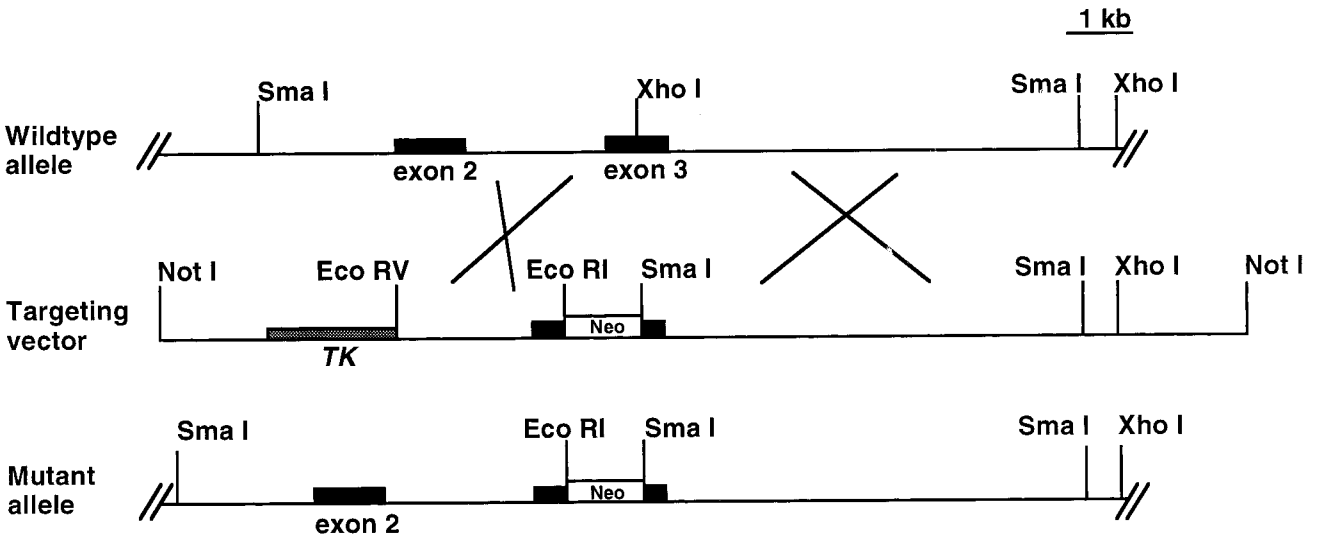

FIG. 1. Diagram of *Irr* targeting vector. Targeted disruption of the *Irr* gene. Restriction map of the *Irr* locus and gene targeting strategy. The pGK-*neo* cassette was introduced into the third exon, therefore disrupting *Irr* transcription. The main restriction enzyme sites are indicated. Abbreviations: Neo, pGK-neomycin gene; *TK*, thymidine kinase gene.

MATERIALS AND METHODS

Gene targeting and generation of *Irr* knockout mice. We used a mouse *Irr* cDNA as a probe to screen a mouse 129 genomic lambda library. Seven overlapping clones covering most of the *Irr* gene were found and subsequently mapped with several restriction enzymes. The targeting construct was made by inserting a pGK-*neo* cassette into the *Xho*I restriction site in the third coding exon of *Irr*. The positive-negative selection method was used, inserting the thymidine kinase gene at the end of the shorter arm of the targeting construct (Fig. 1) (26). The construct was linearized with *Not*I and electroporated into CJ7 embryonic stem (ES) cells. Homologous recombinants were identified by Southern blotting with appropriate 5′- and 3′-flanking probes. Four ES cell clones bearing the desired recombination events were microinjected into E3.5 blastocysts as described (1), and resulting chimeric offspring were tested for germ line transmission by back-crossing onto C57BL/6J.

RT-PCR analysis of IRR gene expression. mRNA was isolated from kidney of $Irr^{-/-}$ and wild-type mice using the Micro-Fast Track 2.0 kit (Invitrogen, Carlsbad, Calif.) and employed to synthesize cDNA using a Gene Amp RNA PCR kit (Perkin-Elmer, Boston, Mass.). PCR was performed using cDNA as a template and amplification primers corresponding to the sequences of exon 2 and exon 4 of *Irr* (forward primer, 5′ ACT GAC TAC AGG TGC TGG ACG 3′; reverse primer, 5′ ACC AGG TCC TGT GTG GCT TGG 3′). PCR amplification conditions were as follows: 2 min at 95°C, followed by 35 cycles at 95°C for 1 min, 60°C for 1 min, and 72°C for 1 min. The last extension cycle was carried out for 7 min. Reaction products were analyzed by agarose gel electrophoresis. The bands corresponding to the *Irr* mRNA product (436 bp) were excised from the gel and sequenced to confirm the mRNA identity.

Western blot analysis of IRR. Western blot analysis was performed with membrane preparations from kidney, liver, or a 293 cell line expressing IRR under the control of a cytomegalovirus promoter. Proteins (30 μg) were separated under nonreducing conditions on a 5 to 20% polyacrylamide gradient gel at 50 A for 4 h and then transferred to a nitrocellulose membrane overnight. The membrane was blocked for 1 h with Tris-buffered saline–Triton X-100 (TBS-T) buffer supplemented with 3% milk and incubated with an antipeptide antibody raised against a synthetic 15-amino-acid peptide corresponding to a fragment of the juxtamembrane domain of IRR (sp-727, 6.6 μg/ml) for 3 h. After incubation with the second antibody (goat anti-rabbit immunoglobulin-horseradish peroxidase conjugate, 1:2,000 dilution) for 1 h and chemiluminescent detection (ECL kit; Amersham), the blot was exposed to X-ray film.

Animal production and genotyping. Mice bearing a null *Ir* allele have been described in previous publications (18). Intercrosses of $Irr^{+/-}$ and $Ir^{+/-}$ mice were used to obtain mice of five genotypes: WT, $Ir^{+/-}$, $Irr^{-/-}$, $Irr^{-/-}$ $Ir^{+/-}$, and $Irr^{-/-}$ $Ir^{-/-}$. Genotyping was performed as follows. The wild-type *Ir* allele was detected using forward primer 5′ TCT TTG CCT GTG CTC CAC TCT 3′ and reverse primer 5′ CTG TGC ACT TCC CTG CTC ACA 3′; the null *Ir* allele was detected using forward primer 5′ TCT TTG CCT GTG CTC CAC TCT 3′ and reverse primer 5′ ATA TTG CTG AAG AGC TTG GCG 3′. The product of the wild-type allele was approximately 100 bp, and that of the null allele was approximately 500 bp. PCR amplification conditions were 4 min at 94°C followed by 30 cycles at 94°C for 1 min, 60°C for 1 min, and 72°C for 1 min, and then 72°C for 7 min. The *Irr* mutant mice were routinely genotyped by PCR. The wild-type allele was detected using oligonucleotides 4856 and 4857, while the mutant allele was detected using oligonucleotides 3202 and 4856 (3202, 5′ CGC CTT CTT GAC GAG TTC TTC TG 3′; 4856, 5′ GTG TGT CCC TGC CCC CGA GGG 3′; 4857, 5′ TGA CAC AGC GCC AGG ACT CAT 3′). The PCR program used consisted of 94°C for 3 min followed by 35 cycles of 94°C for 1 min, 56°C for 1 min, and 72°C for 2 min, followed by a final 5-min extension at 72°C.

Phenotypic analysis. Blood was drawn from the retroorbital sinus of anesthetized adult mice. Only male mice were used in the analysis because they are more prone to insulin resistance. Newborn mice were euthanized by CO_2 followed by cervical dislocation and exsanguinated for glucose and insulin measurements. Blood glucose levels were determined using an Accucheck glucometer from Boehringer Mannheim (Mannheim, Germany). Serum insulin was measured by radioimmunoassay using a rat insulin standard (Linco Research, St. Charles, Mo.). All assays were carried out in duplicate. Each value represents the mean of two independent determinations (18).

Intraperitoneal glucose tolerance test. Mice fasted for 16 h and were anesthetized with pentobarbital (40 mg/kg of body weight). Blood was drawn immediately prior to and 30, 60, 90, and 120 min after intraperitoneal injection of glucose (2 g/kg of body weight) (18). Glucose and insulin levels were measured as described above.

Insulin tolerance test. Mice were fed freely and tested between 2 and 4 p.m. Mice were anesthetized with pentobarbital (40 mg/kg body of weight). Blood samples were drawn immediately prior to and 30 and 60 min after intraperitoneal injection of 0.75 U of human insulin (Sigma) per kg of body weight (0.026 mg/kg). Glucose levels were measured as described above.

Insulin secretion from isolated islets. Islets were isolated from 6-month-old WT, $Irr^{-/-}$, $Irr^{-/-}$ $Ir^{+/-}$, and $Ir^{+/-}$ mice by collagenase digestion followed by centrifugation over a Histopaque gradient. Briefly, after clamping the common bile duct at its entrance to the duodenum, 3 ml of M199 medium containing 1 mg of collagenase P (Roche Molecular Biochemicals, Indianapolis, Ind.) per ml was injected into the duct. The swollen pancreas was surgically removed and incubated at 37°C for 17 min. Thereafter, 30 ml of ice-cold M199 medium containing 10% newborn calf serum (NCS) was added to stop the digestion reaction. Digested pancreata were dispersed by pipetting and rinsed twice with 30 ml of the same medium. After filtering the tissue suspension through a Spectra-mesh (408 μm; Spectrum Laboratories, Inc.), the digested tissue was resuspended in 10 ml of Histopaque and overlaid with 10 ml of M199 medium. The sample was then centrifuged at 1,700 × *g* for 20 min, and the islets were collected from the interface. The recovered material was washed twice with cold M199 medium, resuspended in RPMI medium containing 10% NCS and 5 mM glucose, and

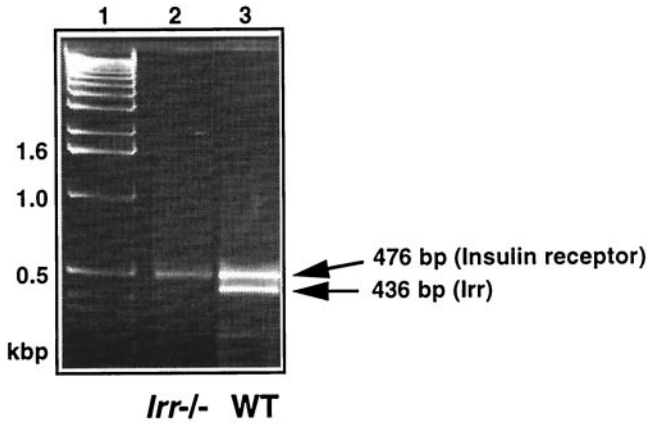

FIG. 2. Detection of *Irr* mRNA by RT-PCR in kidney extracts. RT-PCR analysis was performed on mRNA isolated from kidney of WT and $Irr^{-/-}$ mice using a set of primers in the *Irr* sequence, as described in the text. The size of the expected *Irr* PCR product is indicated. The upper band corresponds to *Ir*. The identity of the two bands was determined by sequence analysis. No PCR product was detected when the reverse transcription step was omitted (data not shown). Lane 1, molecular size markers; lane 2, $Irr^{-/-}$ mice: lane 3, WT mice.

cultured overnight at 37°C in 5% CO_2. For insulin secretion assays, islets were manually picked under a dissection microscope using a pipette, placed in ice-cold Krebs buffer (119 mM NaCl, 2.5 mM $CaCl_2$, 1.19 mM KH_2PO_4, 1.19 mM Mg_2SO_4, 10 mM HEPES [pH 7.4], 2% bovine serum albumin, and 2.8 mM glucose) and incubated at 37°C for 15 min. At the end of the incubation period, islets were stimulated with various glucose concentrations (2.8, 5.6, 11.2, and 16.8 mM) for 1 h at 37°C. At the end of the incubation, the islets were collected by centrifugation and the supernatant was assayed for insulin content by radioimmunoassay (22).

Immunohistochemical and morphometric analysis of pancreatic islets. Pancreata were removed from 4-day-old WT, $Irr^{-/-}$, and $Irr^{-/-}$ $Ir^{-/-}$ mice and fixed overnight in Bouin's solution. Tissues were embedded in paraffin, and consecutive 5-μm sections were mounted on slides. After rehydration and permeabilization in 0.1% Triton X-100, sections were immunostained for β cells using mouse anti-insulin antibodies and for α cells using mouse antiglucagon antibodies (Sigma Chemical Co.). For quantitation of α- and β-cell area, two animals for each genotype were analyzed at postnatal day 4. For each pancreas, 10 sections were covered systematically by accumulating images from nonoverlapping fields. Images were captured with a digital camera (Nikon 950) and analyzed using the NIH Image 1.60 software as described previously (18). Results were expressed as a percentage of the total surveyed pancreatic area occupied by α and β cells.

RESULTS

$Irr^{-/-}$ mice do not express *Irr* mRNA. To generate mice lacking IRR, a nonsense mutation was introduced in exon 3 of murine *Irr* by homologous recombination in mouse ES cells. The targeting strategy is shown in Fig. 1. To confirm that this mutation resulted in the generation of a null *Irr* allele, we performed reverse transcription (RT)-PCR amplification on mRNA isolated from kidney of WT and $Irr^{-/-}$ mice. Kidney was chosen as the organ with the highest levels of *Irr* expression (4, 24, 34). The expected PCR product of 436 bp was detected in WT mice but not in $Irr^{-/-}$ mice (Fig. 2). An additional PCR product of 476 bp was detected in both WT and $Irr^{-/-}$ mice. Sequence analysis indicated that this DNA fragment corresponds to *Ir* mRNA, whereas the lower band corresponds to *Irr* mRNA (data not shown), consistent with the notion that $Irr^{-/-}$ mice do not express *Irr* mRNA.

TABLE 1. Metabolic data for 6-month-old WT, $Ir^{+/-}$, $Irr^{-/-}$, and $Irr^{-/-}$ $Ir^{+/-}$ mice[a]

Genotype (*n*)	Body wt (gm)	Glucose		Insulin	
		Fasting	Fed	Fasting	Fed
WT (15)	35.8 ± 0.7	96 ± 4	135 ± 6	0.7 ± 0.2	2.8 ± 0.8
$Irr^{-/-}$ (20)	36.0 ± 0.8	104 ± 6	139 ± 11	0.5 ± 0.1	3.8 ± 0.6
$Irr^{+/-}$ (16)	34.0 ± 0.8	97 ± 3	132 ± 12	1.4 ± 0.4	8.4 ± 1.2
$Irr^{-/-}$ $Ir^{+/-}$ (21)	34.5 ± 0.9	98 ± 5	134 ± 9	0.8 ± 0.2	9.6 ± 1.6

[a] The data represent the mean ± SEM. Values for individual mice represent the mean of at least two separate determinations. Values for insulin are in nanograms per milliliter; values for glucose are in milligrams per decaliter.

We next examined the expression of IRR protein using antipeptide antibody raised against a synthetic 15-amino-acid peptide corresponding to a fragment of the juxtamembrane domain of the IRRβ subunit (4). Under nonreducing conditions, a 350-kDa peptide corresponding to the heterotetrameric IRR band was detected in WT and $Irr^{+/-}$ mice but not in $Irr^{-/-}$ kidney extract (Fig. 3).These results indicate that the *Irr* protein product is absent in $Irr^{-/-}$ mice.

Phenotypic characterization of mice lacking IRR. $Irr^{-/-}$ mice were born with the expected Mendelian frequency and showed no growth, morphological, or gross behavioral abnormalities (data not shown). To assess the consequences of *Irr* ablation on glucose metabolism, we measured whole-blood glucose and serum insulin levels in the fasting and fed states in 6-month-old WT and $Irr^{-/-}$ mice. No differences were detected between WT and $Irr^{-/-}$ mice (Table 1). Glucose tolerance tests were performed to detect subtle defects in insulin sensitivity that would not result in overt diabetes. However, glucose values following intraperitoneal glucose administration were similar in WT and $Irr^{-/-}$ mice (Fig. 4a). To determine whether the lack of IRR would affect metabolic control in the context of a predisposing background, we crossed $Irr^{-/-}$ mice with insulin-resistant $Ir^{+/-}$ mice (1, 19), which have been

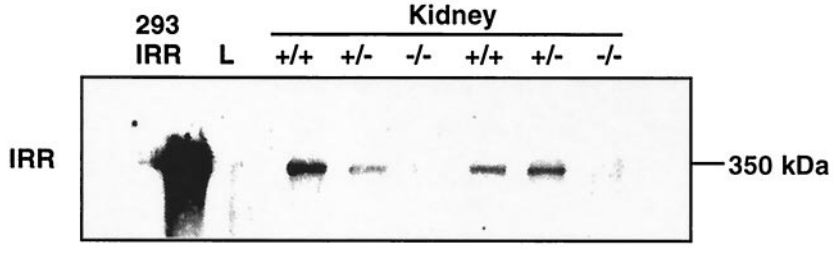

FIG. 3. Western blot analysis of *Irr* expression under nonreducing conditions. Anti-IRR staining reveals a specific band at ~350 kDa corresponding to the heterotetrameric IRR visible in WT and $Irr^{+/-}$ kidney samples but not in $Irr^{-/-}$ mice, indicating that the *Irr* mutant mice carry a bona fide gene knockout. No signal was detected in the negative control (liver, lane L). The positive control used was a protein extract from 293 cells expressing IRR (IRR-293).

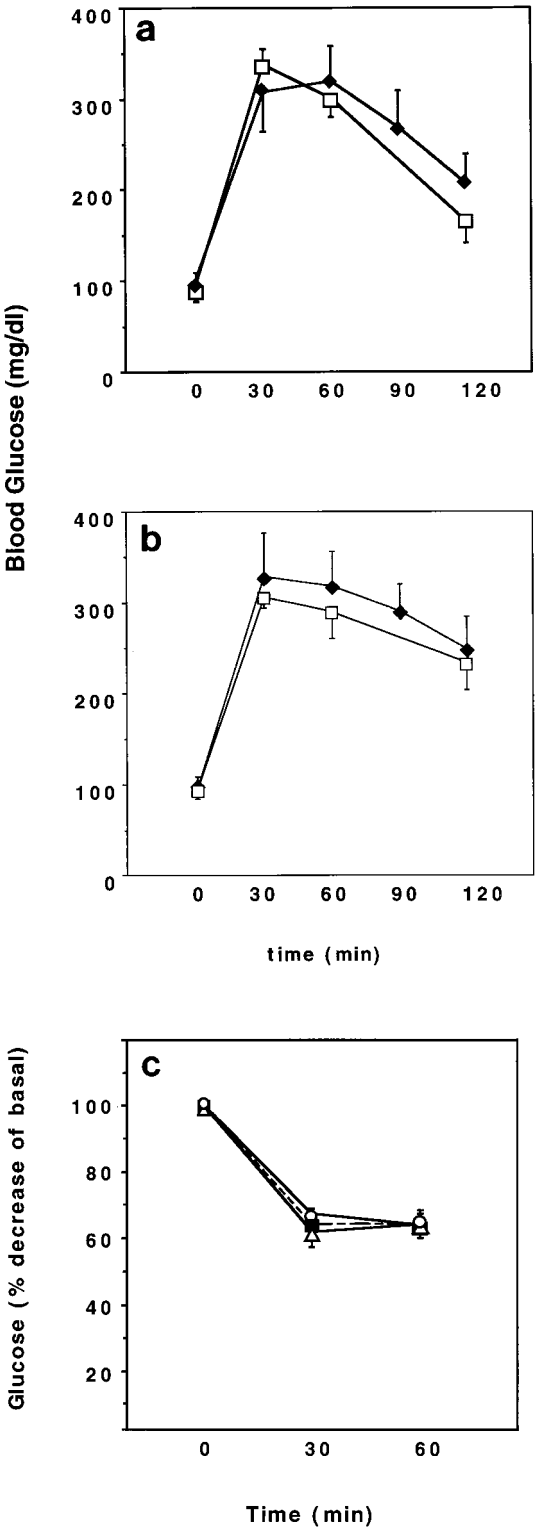

FIG. 4. Glucose and insulin tolerance tests. Glucose (a and b) or insulin (c) were administered by intraperitoneal injections at doses of 2 g/kg and 0.75 U/kg, respectively. Whole-blood glucose values were measured at the indicated time points after the injection. The results represent the mean ± standard error of the mean (SEM) for at least six animals in each group. Symbols: (A) Open squares, WT; solid diamonds, $Irr^{-/-}$; (B) open squares, $Ir^{+/-}$; solid diamonds, $Irr^{-/-}$ $Ir^{+/-}$; (C) open circles, WT; solid squares, $Irr^{-/-}$; open triangles, $Irr^{-/-}$ $Ir^{+/-}$.

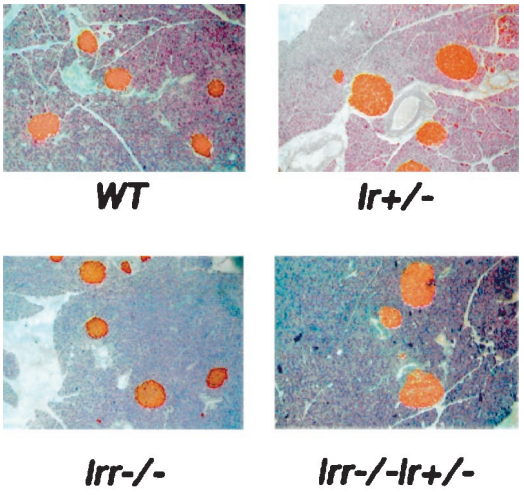

FIG. 5. Insulin immunohistochemistry. Pancreata were obtained from 6-month-old WT, $Ir^{+/-}$, $Irr^{-/-}$, and $Irr^{-/-}$ $Ir^{+/-}$ mice. Insulin immunohistochemistry was performed using a mouse anti-insulin antibody (see text). A representative section is shown for each genotype.

shown to develop diabetes with high frequency when crossed with mice bearing other predisposing mutations (7, 8, 18). $Irr^{-/-}$ $Ir^{+/-}$ mice showed fasting and fed glucose and insulin levels similar to those seen in $Ir^{+/-}$ mice (Table 1). Glucose tolerance tests indicated that $Irr^{-/-}$ $Ir^{+/-}$ mice were as glucose intolerant as $Ir^{+/-}$ mice, suggesting that lack of IRR does not further impair glucose metabolism (Fig. 4b). Insulin tolerance tests failed to demonstrate any difference among WT, $Irr^{-/-}$, and $Irr^{-/-}Ir^{+/-}$ mice (Fig. 4c). We next examined pancreatic islets by immunohistochemistry with anti-insulin antibodies. Islet mass was moderately enlarged in $Ir^{+/-}$ mice (Fig. 5, upper right panel). In contrast, $Irr^{-/-}$ mice had islet mass similar to that of WT controls. In $Irr^{-/-}$ $Ir^{+/-}$ mice, islet mass was similar to that observed in $Ir^{+/-}$ mice (Fig. 5, lower right panel). Morphometric analyses failed to reveal differences between islets from $Irr^{-/-}$ and $Irr^{-/-}$ $Ir^{+/-}$ mice (not shown).

Normal glucose-induced insulin secretion in pancreatic islets isolated from $Irr^{-/-}$ mice. In view of the potential role of IRR in β-cell function, we examined glucose-induced insulin secretion in islets isolated from $Irr^{-/-}$ and $Irr^{-/-}$ $Ir^{+/-}$ mice and compared them with WT islets. As shown in Fig. 6, glucose induced a dose-dependent increase in insulin secretion up to a maximum of ~20-fold over basal at 16.8 mM. Similar secretion patterns were observed in all genotypes examined, which included WT, $Irr^{-/-}$, $Ir^{+/-}$, and $Irr^{-/-}$ $Ir^{+/-}$ mice. These data, along with the data on in vivo glucose tolerance, are consistent with a preserved function of $Irr^{-/-}$ islets to secrete insulin in response to a glucose challenge.

Development of diabetes in *Ir*/*Irr* double-knockout mice. Next, we investigated the possibility that the lack of an overt phenotype in $Irr^{-/-}$ mice may be due to compensation by *Ir*. Thus, double-knockout mice lacking both *Irr* and *Ir* were obtained and characterized. This type of analysis was limited to the immediate postnatal period, since mice lacking *Ir* die within a week of birth. As shown in Fig. 7, plasma glucose and insulin levels rose sharply after birth in $Irr^{-/-}$ $Ir^{-/-}$ mice, similar to $Ir^{-/-}$ mice (1). Double-knockout mice died of dia-

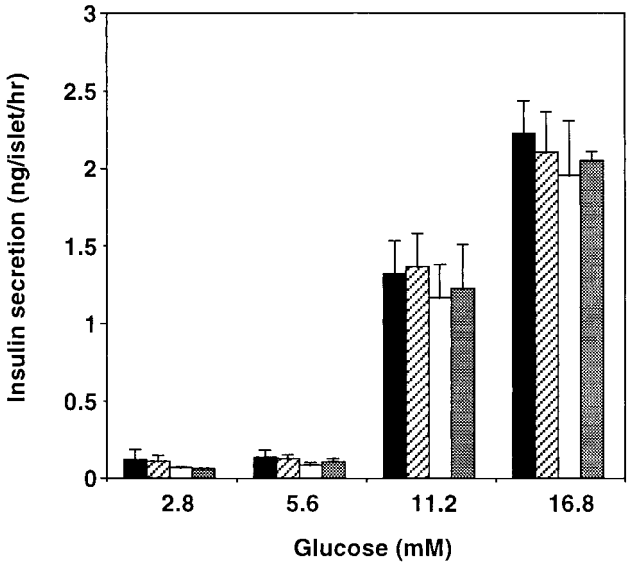

FIG. 6. Insulin secretion from isolated islets. Islets of Langerhans were isolated by in situ perfusion of the pancreas followed by collagenase digestion and Ficoll-Hypaque gradient centrifugation. After overnight culture in 5 mM glucose, islets from WT, $Irr^{-/-}$, $Ir^{+/-}$, and $Irr^{-/-}$ $Ir^{+/-}$ mice were stimulated to release insulin by culturing for 1 h with the indicated glucose concentrations. Results represent the mean ± SEM for four animals in each group. Open bars, WT; solid bars, $Irr^{-/-}$; stippled bars, $Irr^{-/-}$ $Ir^{+/-}$; gray bars, $Ir^{+/-}$.

betic ketoacidosis within 5 days of birth. Thus, ablation of *Irr* did not affect the phenotype of $Ir^{-/-}$ mice.

Islet morphology and analysis of β-cell mass in $Irr^{-/-}$ and $Irr^{-/-}$ $Ir^{-/-}$ double-knockout mice. We next examined α- and β-cell mass and islet morphology in newborn *Irr* and *Ir Irr* knockout mice to detect possible effects of the *Irr* mutation on embryonic development of islets. As shown in Fig. 8, islet morphology was unchanged. β-Cell mass represented ~2.5% and α-cell mass represented ~0.5% of total pancreatic mass in both $Irr^{-/-}$ and $Irr^{-/-}$ $Ir^{-/-}$ mice. These findings are consistent with the conclusion that *Irr* is not required for completion of islet development and early postnatal insulin secretion.

DISCUSSION

An important contribution of mice with targeted gene mutations to our understanding of the pathogenesis of insulin resistance is the notion that insulin/IGF signaling affects β-cell function in multiple ways (15). The current paradigm is that IGF-1Rs promote β-cell growth through IRS-2, whereas IRs contribute to glucose sensing through IRS-1 signaling (11, 22, 23, 25, 36, 38, 47, 48). In this model, it remains unclear how IR and IGF-1R would be protected from rapid ligand-induced internalization, given that they are exposed to very high insulin concentrations.

The presence of IRR in β cells has been demonstrated by two groups using different approaches (10, 31). IRR can potentially participate in β-cell growth and function in two possible ways: by mediating signaling of its own — as yet unknown— ligand, or by engaging in heterodimer formation with IR and/or IGF-1R (13, 20, 49). With respect to the first hypothesis, limited evidence does indeed suggest that IRR signaling in PC-12 cells is qualitatively different from IR signaling, with the former being more tightly associated to activation of MAP kinase and cellular differentiation (17), and the latter being required for cellular proliferation (28, 29). It is thus possible that IRR would have a separate role from IR and IGF-1R and that its inability to bind insulin would protect it from ligand-induced internalization. Alternatively, IRR could participate in the formation of heterodimers composed of an IRR monomer and an IR or IGF-1R monomer. It could be envisioned that such heterodimers could either affect ligand-induced internalization or potentiate signaling by determining substrate selection. A similar mechanism, whereby an orphan receptor can modulate the function of liganded receptors of the same family by engaging in heterodimer formation, has been shown for ErbB2, the orphan receptor of the epidermal growth factor family (5, 9, 30, 37, 45).

The hypothesis tested in these studies was that IRR plays a physiologic role in β cells. The data obtained for $Irr^{-/-}$ mice

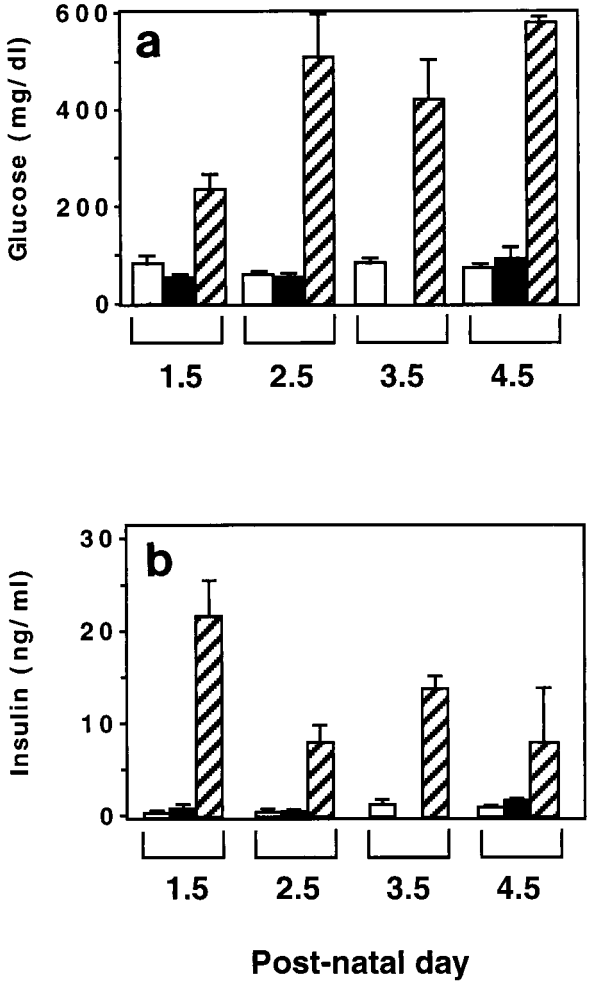

FIG. 7. Metabolic parameters in *Irr Ir*-deficient mice. Blood glucose (a) and serum insulin levels (b) were determined in $Irr^{-/-}$, $Irr^{-/-}$ $Ir^{+/-}$, and $Irr^{-/-}$ $Ir^{-/-}$ littermates at postnatal day 1.5 to 4.5. The results shown represent the mean ± SEM. At each time point, three to five mice for each genotype were analyzed except for $Irr^{-/-}$ mice at day 2 and $Irr^{-/-}$ $Ir^{+/-}$ mice at day 1, when two mice for each genotype were analyzed. Open bars, $Irr^{-/-}$; solid bars, $Irr^{-/-}$ $Ir^{+/-}$; stippled bars, $Irr^{-/-}$ $Ir^{-/-}$.

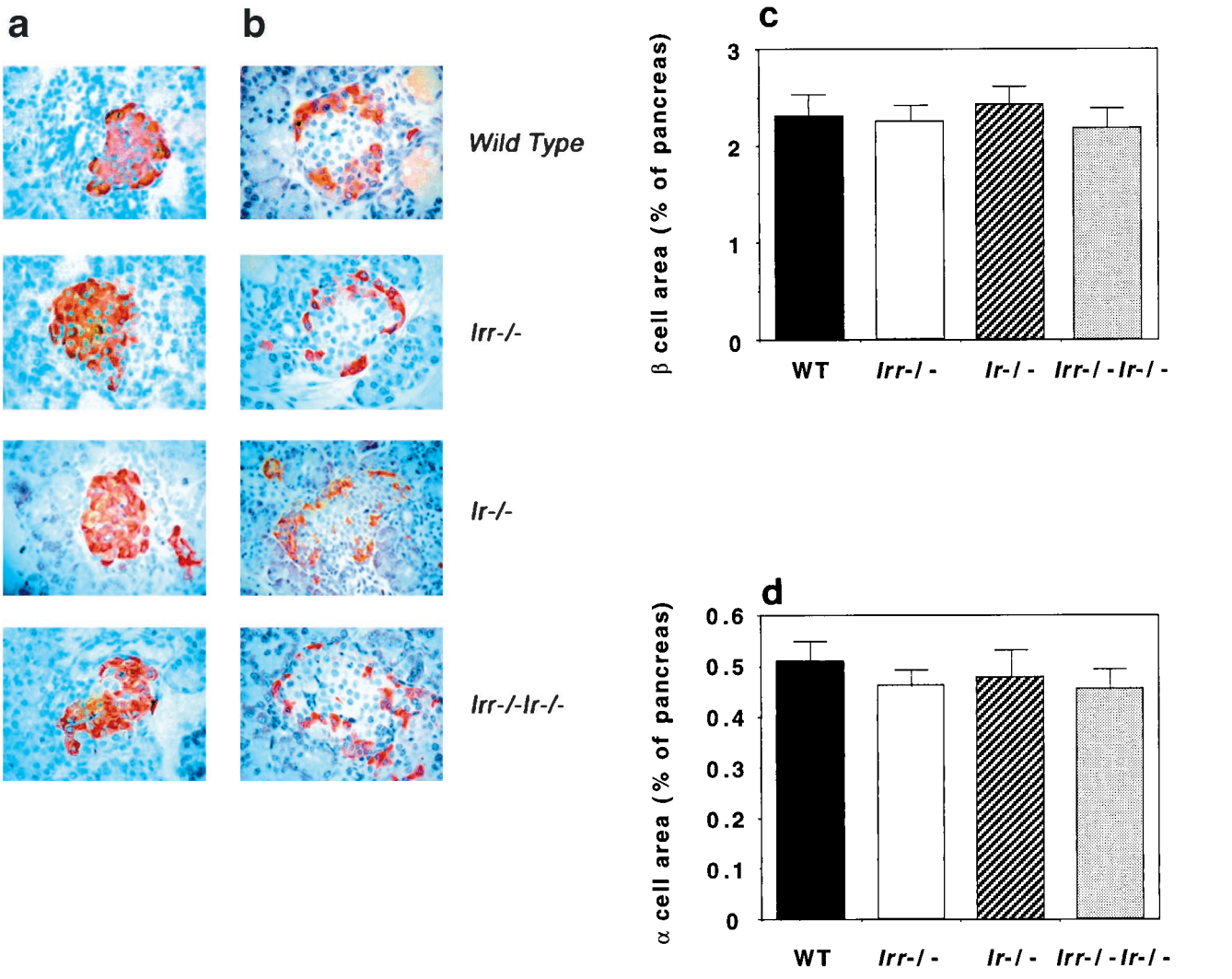

FIG. 8. Islet morphology and analysis of α- and β-cell mass. (a and b) Pancreatic sections from 4-day-old WT, $Irr^{-/-}$, $Ir^{-/-}$, and $Irr^{-/-}$ $Ir^{-/-}$ mice were stained with anti-insulin antibodies (a) and antiglucagon antibodies (b). Representative islets are shown. (c and d) Quantitation of β-cell (c) and α-cell (d) area in animals of the indicated genotype was performed using the NIH Image 1.60 analysis software. Results were expressed as the percentage of the total surveyed area containing insulin-positive or glucagon-positive cells.

clearly disprove this hypothesis. Moreover, the failure of $Irr^{-/-}$ $Ir^{+/-}$ mice to develop either diabetes or more severe insulin resistance also indicates that IRR is not required for β-cell compensation to the mild insulin resistance caused by the *Ir* mutation.

The last hypothesis of our work was that *Irr* is required for embryonic β-cell development and that the lack of phenotype in $Irr^{-/-}$ mice could be explained by the compensatory actions of *Ir* or *Igf1r*. This hypothesis is based on our recent observation that combined ablation of *Ir* and *Igf1r* is compatible with normal embryonic β-cell development (Y. Kido, J. Nakae, S. Xuan, A. Efstratiadis, and D. Accili, Diabetes **49**[Suppl. 1], 2000, abstr. 1066), suggesting that additional growth factor receptors contribute to β-cell growth. However, combined ablations of *Ir* and *Irr* resulted in a phenotype identical to that observed in $Ir^{-/-}$ mice, suggesting that embryonic β-cell development can occur in the absence of *Irr*.

The failure of IRR to partake in β-cell function could be related to the observation of Hirayama and coworkers that β-cell IRR is mostly expressed as an unprocessed polypeptide precursor rather than as cleaved, functionally mature α-β subunits (10). If intracellular processing of IRR occurs by a mechanism similar to IR processing, it is likely that most uncleaved precursor is retained intracellularly and is not expressed at the plasma membrane (2, 3), thus limiting the amount of functional IRR. In conclusion, the present data rule out a contribution by *Irr* to β-cell growth and function and indicate that lack of this orphan receptor does not affect residual IR function in insulin-resistant $Ir^{+/-}$ mice, consistent with the lack of a metabolic role of *Irr* in peripheral tissues.

ACKNOWLEDGMENTS

This work was supported by NIH grants DK58282, DK57539, and JDF 2000-893 to D.A. and by R37NS331999 to L.F.P.

We thank Jun Nakae for helpful comments on the manuscript.

REFERENCES

1. **Accili, D., J. Drago, E. J. Lee, M. D. Johnson, M. H. Cool, P. Salvatore, L. D. Asico, P. A. Jose, S. I. Taylor, and H. Westphal.** 1996. Early neonatal death

in mice homozygous for a null allele of the insulin receptor gene. Nat. Genet. **12:**106–109.
2. **Accili, D., C. Frapier, L. Mosthaf, C. McKeon, S. C. Elbein, M. A. Permutt, E. Ramos, E. Lander, A. Ullrich, and S. I. Taylor.** 1989. A mutation in the insulin receptor gene that impairs transport of the receptor to the plasma membrane and causes insulin-resistant diabetes. EMBO J. **8:**2509–2517.
3. **Accili, D., T. Kadowaki, H. Kadowaki, L. Mosthaf, A. Ullrich, and S. I. Taylor.** 1992. Immunoglobulin heavy chain-binding protein binds to misfolded mutant insulin receptors with mutations in the extracellular domain. J. Biol. Chem. **267:**586–590.
4. **Bates, C. M., J. M. Merenmies, K. S. Kelly-Spratt, and L. F. Parada.** 1997. Insulin receptor-related receptor expression in non-A intercalated cells in the kidney. Kidney Int. **52:**674–681.
5. **Beerli, R. R., D. Graus-Porta, K. Woods-Cook, X. Chen, Y. Yarden, and N. E. Hynes.** 1995. Neu differentiation factor activation of ErbB-3 and ErbB-4 is cell specific and displays a differential requirement for ErbB-2. Mol. Cell. Biol. **15:**6496–6505.
6. **Bonner-Weir, S.** 2000. Life and death of the pancreatic beta cells. Trends Endocrinol. Metab. **11:**375–378.
7. **Bruning, J. C., M. D. Michael, J. N. Winnay, T. Hayashi, D. Horsch, D. Accili, L. J. Goodyear, and C. R. Kahn.** 1998. A muscle-specific insulin receptor knockout exhibits features of the metabolic syndrome of NIDDM without altering glucose tolerance. Mol. Cell **2:**559–569.
8. **Bruning, J. C., J. Winnay, W. S. Bonner, S. I. Taylor, D. Accili, and C. R. Kahn.** 1997. Development of a novel polygenic model of NIDDM in mice heterozygous for IR and IRS-1 null alleles. Cell **88:**561–572.
9. **Graus-Porta, D., R. R. Beerli, J. M. Daly, and N. E. Hynes.** 1997. ErbB-2, the preferred heterodimerization partner of all ErbB receptors, is a mediator of lateral signaling. EMBO J. **16:**1647–1655.
10. **Hirayama, I., H. Tamemoto, H. Yokota, S. K. Kubo, J. Wang, H. Kuwano, Y. Nagamachi, T. Takeuchi, and T. Izumi.** 1999. Insulin receptor-related receptor is expressed in pancreatic beta-cells and stimulates tyrosine phosphorylation of insulin receptor substrate-1 and -2. Diabetes **48:**1237–1244.
11. **Hugl, S. R., M. F. White, and C. J. Rhodes.** 1998. Insulin-like growth factor I (IGF-I)-stimulated pancreatic beta-cell growth is glucose-dependent. Synergistic activation of insulin receptor substrate-mediated signal transduction pathways by glucose and IGF-I in INS-1 cells. J. Biol. Chem. **273:**17771–17779.
12. **Itoh, N., K. Jobo, K. Tsujimoto, M. Ohta, and T. Kawasaki.** 1993. Two truncated forms of rat insulin receptor-related receptor. J. Biol. Chem. **268:**17983–17986.
13. **Jui, H. Y., D. Accili, and S. I. Taylor.** 1996. Characterization of a hybrid receptor formed by dimerization of the insulin receptor-related receptor (IRR) with the insulin receptor (IR): coexpression of cDNAs encoding human IRR and human IR in NIH-3T3 cells. Biochemistry **35:**14326–14330.
14. **Jui, H. Y., Y. Suzuki, D. Accili, and S. I. Taylor.** 1994. Expression of a cDNA encoding the human insulin receptor-related receptor. J. Biol. Chem. **269:** 22446–22452.
15. **Kadowaki, T.** 2000. Insights into insulin resistance and type 2 diabetes from knockout mouse models. J. Clin. Investig. **106:**459–465.
16. **Kahn, B. B.** 1998. Type 2 diabetes: when insulin secretion fails to compensate for insulin resistance. Cell **92:**593–596.
17. **Kelly-Spratt, K. S., L. J. Klesse, J. Merenmies, and L. F. Parada.** 1999. A TrkB/insulin receptor-related receptor chimeric receptor induces PC12 cell differentiation and exhibits prolonged activation of mitogen-activated protein kinase. Cell Growth Differ. **10:**805–812.
18. **Kido, Y., D. J. Burks, D. Withers, J. C. Bruning, C. R. Kahn, M. F. White, and D. Accili.** 2000. Tissue-specific insulin resistance in mice with combined mutations of insulin receptor, IRS-1 and IRS-2. J. Clin. Investig. **105:**199–205.
19. **Kido, Y., N. Philippe, A. A. Schaeffer, and D. Accili.** 2000. Genetic modifiers of the insulin resistance phenotype. Diabetes **49:**589–596.
20. **Kovacina, K. S., and R. A. Roth.** 1995. Characterization of the endogenous insulin receptor-related receptor in neuroblastomas. J. Biol. Chem. **270:** 1881–1887.
21. **Kubota, N., K. Tobe, Y. Terauchi, K. Eto, T. Yamauchi, R. Suzuki, Y. Tsubamoto, K. Komeda, R. Nakano, H. Miki, S. Satoh, H. Sekihara, S. Sciacchitano, M. Lesniak, S. Aizawa, R. Nagai, S. Kimura, Y. Akanuma, S. I. Taylor, and T. Kadowaki.** 2000. Disruption of insulin receptor substrate 2 causes type 2 diabetes because of liver insulin resistance and lack of compensatory beta-cell hyperplasia. Diabetes **49:**1880–1889.
22. **Kulkarni, R. N., J. C. Bruning, J. N. Winnay, C. Postic, M. A. Magnuson, and C. R. Kahn.** 1999. Tissue-specific knockout of the insulin receptor in pancreatic beta cells creates an insulin secretory defect similar to that in type 2 diabetes. Cell **96:**329–339.
23. **Kulkarni, R. N., J. N. Winnay, M. Daniels, J. C. Bruning, S. N. Flier, D. Hanahan, and C. R. Kahn.** 1999. Altered function of insulin receptor substrate-1-deficient mouse islets and cultured beta-cell lines. J. Clin. Investig. **104:**R69–R75.
24. **Kurachi, H., K. Jobo, M. Ohta, T. Kawasaki, and N. Itoh.** 1992. A new member of the insulin receptor family, insulin receptor-related receptor, is expressed preferentially in the kidney. Biochem. Biophys. Res. Commun. **187:**934–939.
25. **Leibiger, I. B., B. Leibiger, T. Moede, and P. O. Berggren.** 1998. Exocytosis of insulin promotes insulin gene transcription via the insulin receptor/PI-3 kinase/p70 s6 kinase and CaM kinase pathways. Mol. Cell **1:**933–938.
26. **Mansour, S. L., K. R. Thomas, and M. R. Capecchi.** 1988. Disruption of the proto-oncogene int-2 in mouse embryo-derived stem cells: a general strategy for targeting mutations to non-selectable genes. Nature **336:**348–352.
27. **Mathi, S. K., J. Chan, and V. M. Watt.** 1995. Insulin receptor-related receptor messenger ribonucleic acid: quantitative distribution and localization to subpopulations of epithelial cells in stomach and kidney. Endocrinology **136:**4125–4132.
28. **Nielsen, F. C., and S. Gammeltoft.** 1988. Insulin-like growth factors are mitogens for rat pheochromocytoma PC 12 cells. Biochem. Biophys. Res. Commun. **154:**1018–1023.
29. **Ohmichi, M., L. Pang, V. Ribon, and A. R. Saltiel.** 1993. Divergence of signaling pathways for insulin in PC-12 pheochromocytoma cells. Endocrinology **133:**46–56.
30. **Olayioye, M. A., R. M. Neve, H. A. Lane, and N. E. Hynes.** 2000. The ErbB signaling network: receptor heterodimerization in development and cancer. EMBO J. **19:**3159–3167.
31. **Ozaki, K.** 1998. Insulin receptor-related receptor in rat islets of Langerhans. Eur. J. Endocrinol. **139:**244–247.
32. **Ozaki, K., N. Takada, K. Tsujimoto, N. Tsuji, T. Kawamura, E. Muso, M. Ohta, and N. Itoh.** 1997. Localization of insulin receptor-related receptor in the rat kidney. Kidney Int. **52:**694–698.
33. **Polonsky, K. S., J. Sturis, and G. I. Bell.** 1996. Non-insulin-dependent diabetes mellitus—a genetically programmed failure of the beta cell to compensate for insulin resistance. N. Engl. J. Med. **334:**777–783.
34. **Reinhardt, R. R., E. Chin, B. Zhang, R. A. Roth, and C. A. Bondy.** 1993. Insulin receptor-related receptor messenger ribonucleic acid is focally expressed in sympathetic and sensory neurons and renal distal tubule cells. Endocrinology **133:**3–10.
35. **Reinhardt, R. R., E. Chin, B. Zhang, R. A. Roth, and C. A. Bondy.** 1994. Selective coexpression of insulin receptor-related receptor (IRR) and TRK in NGF-sensitive neurons. J. Neurosci. **14:**4674–4683.
36. **Rhodes, C. J.** 2000. IGF-I and GH post-receptor signaling mechanisms for pancreatic beta- cell replication. J. Mol. Endocrinol. **24:**303–311.
37. **Schlessinger, J.** 2000. Cell signaling by receptor tyrosine kinases. Cell **103:** 211–225.
38. **Schuppin, G. T., S. Pons, S. Hugl, L. P. Aiello, G. L. King, M. White, and C. J. Rhodes.** 1998. A specific increased expression of insulin receptor substrate 2 in pancreatic beta-cell lines is involved in mediating serum-stimulated beta-cell growth. Diabetes **47:**1074–1085.
39. **Shier, P., and V. M. Watt.** 1989. Primary structure of a putative receptor for a ligand of the insulin family. J. Biol. Chem. **264:**14605–14608.
40. **Shier, P., and V. M. Watt.** 1992. Tissue-specific expression of the rat insulin receptor-related receptor gene. Mol. Endocrinol. **6:**723–729.
41. **Taylor, S. I.** 1999. Deconstructing type 2 diabetes. Cell **97:**9–12.
42. **Tsuji, N., K. Tsujimoto, N. Takada, K. Ozaki, M. Ohta, and N. Itoh.** 1996. Expression of insulin receptor-related receptor in the rat brain examined by in situ hybridization and immunohistochemistry. Brain Res. Mol. Brain Res. **41:**250–258.
43. **Tsujimoto, K., N. Tsuji, K. Ozaki, M. Minami, M. Satoh, and N. Itoh.** 1995. Expression of insulin receptor-related receptor mRNA in the rat brain is highly restricted to forebrain cholinergic neurons. Neurosci. Lett.**188:**105–108.
44. **Tsujimoto, K., N. Tsuji, K. Ozaki, M. Ohta, and N. Itoh.** 1995. Insulin receptor-related receptor messenger ribonucleic acid in the stomach is focally expressed in the enterochromaffin-like cells. Endocrinology **136:**558–561.
45. **Tzahar, E., R. Pinkas-Kramarski, J. D. Moyer, L. N. Klapper, I. Alroy, G. Levkowitz, M. Shelly, S. Henis, M. Eisenstein, B. J. Ratzkin, M. Sela, G. C. Andrews, and Y. Yarden.** 1997. Bivalence of EGF-like ligands drives the ErbB signaling network. EMBO J. **16:**4938–4950.
46. **Weiner, H. L., M. Rothman, D. C. Miller, and E. B. Ziff.** 1996. Pediatric brain tumors express multiple receptor tyrosine kinases including novel cell adhesion kinases. Pediatr. Neurosurg. **25:**64–72.
47. **Withers, D. J., D. J. Burks, H. H. Towery, S. L. Altamuro, C. L. Flint, and M. F. White.** 1999. Irs-2 coordinates Igf-1 receptor-mediated beta-cell development and peripheral insulin signalling. Nat. Genet. **23:**32–40.
48. **Withers, D. J., J. Sanchez-Gutierrez, H. Towery, D. J. Burks, J.-M. Ren, S. Previs, Y. Zhang, D. Bernal, S. Pons, G. I. Shulman, S. Bonner-Weir, and M. F. White.** 1998. Disruption of IRS-2 causes type 2 diabetes in mice. Nature **391:**900–904.
49. **Zhang, B., and R. A. Roth.** 1992. The insulin receptor-related receptor. Tissue expression, ligand binding specificity, and signaling capabilities. J. Biol. Chem. **267:**18320–18328.
50. **Zhao, A. Z., H. Zhao, J. Teague, W. Fujimoto, and J. A. Beavo.** 1997. Attenuation of insulin secretion by insulin-like growth factor 1 is mediated through activation of phosphodiesterase 3B. Proc. Natl. Acad. Sci. USA **94:**3223–3228.